Binary Maximal-Ratio Combining

Constantin SIRITEANU* and Yoshikazu MIYANAGA†
* Hokkaido University, Sapporo, Japan
E-mail: costi@icn.ist.hokudai.ac.jp, Tel.: +81-11-706-6490/Fax: +81-11-706-7121
† Hokkaido University, Sapporo, Japan
E-mail: miya@ist.hokudai.ac.jp, Tel.: +81-11-706-6489/Fax: +81-11-706-7121

***Abstract*—This paper evaluates the performance of single-input/multiple-output (SIMO) wireless communications systems with binary combining vectors for maximum-ratio combining (MRC). Unlike recent work by other researchers who employed BPSK-like-modulated (i.e., ± 1-valued) vectors for MIMO transmit beamforming, we employ $0/1$-valued vectors, for SIMO MRC. Thus, for highly correlated antennas in Rician and Rayleigh fading, such binary MRC is found nearly as effective as MRC using a channel gain vector estimated based on the minimum mean square error (MMSE) criterion. Furthermore, binary MRC is less demanding than MMSE-based MRC because it does not require signal-to-noise ratio knowledge or matrix inversion. We also find that BPSK-like modulation prevents binary MRC from achieving performance similar to that of MMSE-based MRC. Finally, we determine that for binary MRC it is crucial to transform the matrix with the binary combiners according to the channel statistics.**

I. INTRODUCTION

Wireless communications systems employing multiple-antenna-based transceivers have been shown theoretically to boost performance [1]. However, conventional implementations require high volumes of memory and digital signal processing [2] [3] [4], substantial feedback from the receiver to the transmitter [5], as well as suitable propagation conditions [6] [7] [8] [9]. In this paper, we limit ourselves to the single-input/multiple-output (SIMO) case and study various conventional implementations of maximal-ratio combining (MRC) as well as a novel binary-combining approach that may achieve optimum performance and reduce complexity. Nevertheless, the concepts and methods described herein can be extended to MISO systems [10] and MIMO systems [11] with limited receiver–transmitter feedback. They have been devised for multi-antenna-based orthogonal frequency-division multiplexing (OFDM) systems, e.g., WiFi, LTE, and WiMAX.

In a recent paper on MIMO transmit beamforming with limited feedback, for uncorrelated Rayleigh fading [11], Kim&Beaulieu propose replacing the conventional Grassmannian line packing (GLP) design procedure for the beamforming codebook with a novel procedure based on BPSK-modulating a Hamming block code that is thus found to yield the same performance as GLP codebooks, which are difficult to design. The binary approach can also greatly reduce precoder-related memory storage requirements.

Herein, we pick up on the binary-combiner idea from [11] and evaluate binary MRC employing $0/1$ combiner entries versus conventional pilot-based approaches, for SIMO. Also, we consider the general case of correlated Rician fading, which is more realistic, according to the WINNER II measurements and modeling [12]. Finally, for correlated fading we transform the binary combiner according to the channel correlation matrix, as proposed in [13].

Thus, binary MRC average error rate (AER) performance is shown to approach that of MRC using as combiner the unquantized minimum mean square error (MMSE) channel vector estimate, i.e., MMSE-based MRC for some propagation conditions. Note that, MMSE-based MRC may require more information and computations than the proposed binary MRC. We also find that the binary MRC approach with ± 1-valued combiners from [11] may not help MRC achieve performance similar to that of MMSE-based MRC.

This paper is organized as follows. Section II introduces the signal and channel models. Section III describes the ideal, conventional pilot-based, and new binary MRC approaches. Finally, Section IV shows numerical simulation results.

II. SIGNAL AND CHANNEL MODELS

Consider a mobile station that transmits through a frequency-flat fading channel. At an N_{R}-element base-station antenna array the received signal vector after demodulation, matched-filtering, and symbol-rate sampling is [6]

$$\mathbf{y} = \sqrt{E_{\mathrm{s}}}\; s\; \mathbf{h} + \mathbf{n}, \tag{1}$$

where E_{s} is the average per-symbol transmitted energy, and s is the unit-average-energy transmitted symbol from a constellation with M symbols (e.g., M-PSK, M-QAM). Channel-fading and receiver-noise vectors are described by $\mathbf{h} \sim \mathcal{N}_{\mathrm{c}}(\mathbf{h}_{\mathrm{d}}, \tilde{\mathbf{R}})$ and $\mathbf{n} \sim \mathcal{N}_{\mathrm{c}}(\mathbf{0}, N_0\, \mathbf{I}_{N_{\mathrm{R}}})$, respectively, where N_0 is the noise variance for each antenna, and $\mathbf{I}_{N_{\mathrm{R}}}$ is the $N_{\mathrm{R}} \times N_{\mathrm{R}}$ identity matrix.

When the channel vector elements, h_l, $l = 1 : N_{\mathrm{R}}$, have zero mean, due to diffuse propagation, their absolute values, $|h_l|$, have Rayleigh distribution [14, Eqn. (2.6), p. 18]. When the channel vector elements have nonzero mean, due to specular propagation, their absolute values have Rician distribution [14, Eqn. (2.15), p. 21].

Propagation conditions determine the specular, i.e., deterministic, component $\mathbf{h}_{\mathrm{d}}$ of the channel gain vector and the correlation matrix of the random component $\mathbf{h}_{\mathrm{r}}$, as described in [1, Section 3.4.2] [12]. The Rician K-factor is the power ratio of the deterministic (i.e., the mean) and random components of the channel gain [1, Section 3.4.2]. Assuming equal K for

all antennas, the channel gain vector is:

$$\mathbf{h} = \mathbf{h}_{\rm d} + \mathbf{h}_{\rm r} = \sqrt{\frac{K}{K+1}}\,\mathbf{h}_{\rm d,n} + \sqrt{\frac{1}{K+1}}\,\mathbf{h}_{\rm r,n}, \tag{2}$$

where, without loss of generality, the elements of $\mathbf{h}_{\rm d,n}$ and $\mathbf{h}_{\rm r,n}$ are assumed to be normalized, i.e., $|h_{{\rm d,n},l}| = 1$ and $\mathbb{E}\{|h_{{\rm r,n},l}|^2\} = 1$, respectively, so that $\mathbb{E}\{|h_l|^2\} = 1$. Then, at detection, the average per-symbol signal-to-noise ratio (SNR) is given by $\gamma_{\rm s} = \frac{E_{\rm s}}{N_0}\mathbb{E}\{|h_l|^2\} = \frac{E_{\rm s}}{N_0}$.

The deterministic channel-gain-vector component (i.e., the mean) is given by:

$$\mathbb{E}\{\mathbf{h}\} = \mathbf{h}_{\rm d} = \sqrt{\frac{K}{K+1}}\,\mathbf{h}_{\rm d,n}. \tag{3}$$

Its normalized version $\mathbf{h}_{\rm d,n}$ can be computed as the steering vector corresponding to the line-of-sight (LOS) angle of arrival (AOA) $\theta_{\rm LOS}$. The distribution of the normalized random component is completely described by its correlation matrix, $\mathbf{R} = \mathbb{E}\{\mathbf{h}_{\rm r,n}\,\mathbf{h}_{\rm r,n}^{\mathcal{H}}\}$. This correlation matrix can be computed for realistic Laplacian power azimuth spread (PAS) [12] as a function of the PAS azimuth spread (AS) and central AOA $\theta_{\rm C}$ (ALSO ASSUMED), as well as the antenna interelement distance relative to the carrier wavelength [15]. Then,

$$\widetilde{\mathbf{R}} = \mathbb{E}\left\{ (\mathbf{h} - \mathbf{h}_{\rm d})\ (\mathbf{h} - \mathbf{h}_{\rm d})^{\mathcal{H}} \right\} = \frac{1}{K+1}\,\mathbf{R}. \tag{4}$$

Let us also define the correlation matrix of the channel gain vector $\mathbf{C} = \mathbb{E}\{\mathbf{h}\,\mathbf{h}^{\mathcal{H}}\}$, given by:

$$\mathbf{C} = \frac{K}{K+1}\mathbf{h}_{\rm d,n}\mathbf{h}_{\rm d,n}^{\mathcal{H}} + \frac{1}{K+1}\mathbf{R}. \tag{5}$$

For the rest of the paper the following are assumed perfectly known: channel-vector mean, $\mathbf{h}_{\rm d}$, K-factor, covariance matrix, $\mathbf{R}$, and noise variance, N_0. These channel and noise statistics can, in practice, be estimated accurately since they fluctuate very slowly compared to Doppler-induced multipath fading [16] [6]. Also, since their estimation can be distributed over long intervals, it does not significantly increase the numerical complexity of combining methods employing these estimates [17].

III. Maximal-Ratio Combining (MRC)

A. Combining and Signal Detection

Given the received signal vector $\mathbf{y}$ from (1), an estimate $\widehat{\mathbf{h}}$ of the channel gain vector $\mathbf{h}$, and a linear combiner $\mathbf{w}$, the transmitted symbol s is detected, in general, by mapping

$$\widehat{s} \;=\; \frac{1}{\sqrt{E_{\rm s}}}\frac{\mathbf{w}^{\mathcal{H}}\mathbf{y}}{\mathbf{w}^{\mathcal{H}}\widehat{\mathbf{h}}} = \underbrace{\frac{\mathbf{w}^{\mathcal{H}}\mathbf{h}}{\mathbf{w}^{\mathcal{H}}\widehat{\mathbf{h}}}}_{\alpha}\,s + \underbrace{\frac{1}{\sqrt{E_{\rm s}}}\frac{\mathbf{w}^{\mathcal{H}}\mathbf{n}}{\mathbf{w}^{\mathcal{H}}\widehat{\mathbf{h}}}}_{n} \tag{6}$$

$$\;=\; \alpha\,s + n \tag{7}$$

into the modulation constellation. The operations in (6) compensate for transmit energy ($\frac{1}{\sqrt{E_{\rm s}}}$) and channel fading ($\frac{\mathbf{w}^{\mathcal{H}}\mathbf{y}}{\mathbf{w}^{\mathcal{H}}\widehat{\mathbf{h}}}$). However, note that since $\mathbf{w}^{\mathcal{H}}\widehat{\mathbf{h}}$ is typically real-valued (because $\mathbf{w}$ is typically computed as $\mathbf{w} = \mathbf{A}\,\widehat{\mathbf{h}}$, where $\mathbf{A}$ is some estimation-method-dependent Hermitian matrix, normalization with $\frac{1}{\sqrt{E_{\rm s}}}\frac{1}{\mathbf{w}^{\mathcal{H}}\widehat{\mathbf{h}}}$ is not required for PSK modulation. Note also that $\alpha \approx 1$ for accurate channel estimation, and that the variance of n is inversely proportional to $E_{\rm s}/N_0$.

By averaging over the noise vector $\mathbf{n}$, the SNR for the symbol-detection problem from (6)-(7) is:

$$\gamma = \frac{|\alpha|^2}{\mathbb{E}_{\mathbf{n}}\left[|n|^2\right]} = \frac{E_{\rm s}\,\frac{|\mathbf{w}^{\mathcal{H}}\mathbf{h}|^2}{|\mathbf{w}^{\mathcal{H}}\widehat{\mathbf{h}}|^2}}{\frac{\mathbb{E}_{\mathbf{n}}[|\mathbf{w}^{\mathcal{H}}\mathbf{n}|^2]}{|\mathbf{w}^{\mathcal{H}}\widehat{\mathbf{h}}|^2}} = \frac{E_{\rm s}}{N_0}\frac{|\mathbf{w}^{\mathcal{H}}\mathbf{h}|^2}{\|\mathbf{w}\|^2}. \tag{8}$$

B. Ideal MRC

Given perfect knowledge of the channel gain vector $\mathbf{h}$, the combiner $\mathbf{w}$ that maximizes the SNR in (8) is given by:

$$\mathbf{w}_{\rm MRC,ideal} = \mathbf{h}. \tag{9}$$

Combining $\mathbf{y}$ with $\mathbf{w}_{\rm MRC,ideal}$ is referred to as maximal-ratio combining (MRC). Then, the symbol is estimated by appropriately mapping

$$\widehat{s}_{\rm MRC,ideal} = \frac{1}{\sqrt{E_{\rm s}}}\frac{\mathbf{w}_{\rm MRC,ideal}^{\mathcal{H}}\mathbf{y}}{\mathbf{w}_{\rm MRC,ideal}^{\mathcal{H}}\mathbf{h}} \tag{10}$$

into the modulation constellation.

C. Simple, Pilot-Based MRC

In practice, the channel gain vector $\mathbf{h}$ is estimated from pilot samples. For example, if the pilot symbol (i.e., known at the receiver) $s = 1$ is transmitted, the received pilot sample is

$$\mathbf{y}_{\rm p} = \sqrt{E_{\rm s}}\mathbf{h} + \mathbf{n}, \tag{11}$$

and the simplest estimate of the channel gain vector $\mathbf{h}$ is:

$$\widehat{\mathbf{h}}_{\rm p} = \frac{\mathbf{y}_{\rm p}}{\sqrt{E_{\rm s}}} = \mathbf{h} + \frac{1}{\sqrt{E_{\rm s}}}\,\mathbf{n}. \tag{12}$$

Then, the typical MRC-like combining approach employs [18]

$$\mathbf{w}_{\rm MRC,pilot} = \widehat{\mathbf{h}}_{\rm p}, \tag{13}$$

and the symbol s is estimated by appropriately mapping

$$\widehat{s}_{\rm MRC,pilot} = \frac{1}{\sqrt{E_{\rm s}}}\frac{\mathbf{w}_{\rm MRC,pilot}^{\mathcal{H}}\mathbf{y}}{\mathbf{w}_{\rm MRC,pilot}^{\mathcal{H}}\widehat{\mathbf{h}}_{\rm p}} \tag{14}$$

into the modulation constellation.

D. MMSE MRC

Above, we have solely employed instantaneous channel knowledge, through $\widehat{\mathbf{h}}_{\rm p}$. Given statistical knowledge about channel fading and receiver noise, the channel gain vector can be estimated optimally with the minimum mean square error (MMSE) approach. The MMSE estimate is given by [15]:

$$\widehat{\mathbf{h}}_{\rm MMSE} = \mathbf{G}^{\mathcal{H}}\,\widehat{\mathbf{h}}_{\rm p}, \tag{15}$$

where the $N_{\rm R} \times N_{\rm R}$ matrix $\mathbf{G}$ is given by:

$$\mathbf{G} \;=\; \left[\mathbb{E}\{\widehat{\mathbf{h}}_{\rm p}\,\widehat{\mathbf{h}}_{\rm p}^{\mathcal{H}}\}\right]^{-1}\,\mathbb{E}\{\widehat{\mathbf{h}}_{\rm p}\,\mathbf{h}^{\mathcal{H}}\}$$

$$\;=\; \left[\mathbf{C} + \frac{1}{E_{\rm s}/N_0}\,\mathbf{I}_{N_{\rm R}}\right]^{-1}\,\mathbf{C}. \tag{16}$$

The computation of this $\mathbf{G}$ requires knowledge of $\mathbf{C}$ and $\frac{E_s}{N_0}$. Also, it requires the inversion of a matrix (which may be inaccurate for high SNR and high correlation) and a multiplication of two matrices. Finally, $\mathbf{G}$ requires memory storage space for its ${N_\mathrm{R}}^2$ complex-valued elements. Thus, if real and imaginary parts are represented on 8 bits and $N_\mathrm{R} = 4$, storing $\mathbf{G}$ requires $4^2 \cdot 2 \cdot 8 = 256$ bits. Many such matrices may have to be stored for an OFDM system with many subcarriers.

Then, the MMSE-based MRC combiner is:

$$\mathbf{w}_{\mathrm{MRC,MMSE}} = \widehat{\mathbf{h}}_{\mathrm{MMSE}}, \tag{17}$$

and the symbol s is estimated by appropriately mapping

$$\widehat{s}_{\mathrm{MRC,MMSE}} = \frac{1}{\sqrt{E_\mathrm{s}}} \frac{\mathbf{w}_{\mathrm{MRC,MMSE}}^{\mathcal{H}} \mathbf{y}}{\mathbf{w}_{\mathrm{MRC,MMSE}}^{\mathcal{H}} \widehat{\mathbf{h}}_{\mathrm{MMSE}}} \tag{18}$$

into the modulation constellation. This approach is herein referred to as MMSE MRC.

E. Binary MRC

Let us assume that the receiver maintains an $N_\mathrm{R} \times N$ matrix $\mathbf{W}$ with N binary-valued $N_\mathrm{R} \times 1$ combiners for MRC. (For an OFDM system, this same $\mathbf{W}$ would be used at all subcarriers, as shown below.) Numerical results will be shown for $N_\mathrm{R} = 4$ and $N = 8, 16$.

The first matrix $\mathbf{W}$ for which numerical results are shown later is the 4×8 matrix

$$\mathbf{W}_\mathrm{b} = \begin{pmatrix} 0 & 0 & 0 & 0 & 0 & 0 & 0 & 0 \\ 0 & 0 & 0 & 0 & 1 & 1 & 1 & 1 \\ 0 & 0 & 1 & 1 & 0 & 0 & 1 & 1 \\ 0 & 1 & 0 & 1 & 0 & 1 & 0 & 1 \end{pmatrix}, \tag{19}$$

Such matrix was proposed for limited-feedback-based transmit beamforming in [11]. Note that in [11] this matrix was obtained from a (4, 4) Hamming block code. Storing $\mathbf{W}_\mathrm{b}$ in memory would require $4 \cdot 8 = 32$ bits. Such matrix could also easily be generated every time it is needed.

Numerical results will also be shown for the 4×16 matrix whose first 8 columns are given by $\mathbf{W}_\mathrm{b}$ and last 8 columns are given by:

$$\mathbf{W}_\mathrm{a}(:, 9:16) = \begin{pmatrix} 1 & 1 & 1 & 1 & 1 & 1 & 1 & 1 \\ 0 & 0 & 0 & 0 & 1 & 1 & 1 & 1 \\ 0 & 0 & 1 & 1 & 0 & 0 & 1 & 1 \\ 0 & 1 & 0 & 1 & 0 & 1 & 0 & 1 \end{pmatrix}. \tag{20}$$

Notice that $\mathbf{W}_\mathrm{a}$ comprises all possible 4-tuples, whereas $\mathbf{W}_\mathrm{b}$ comprises all 4-tuples that start with a 0. Storing $\mathbf{W}_\mathrm{a}$ in memory would require $4 \cdot 16 = 64$ bits. Such matrix could also easily be generated every time it is needed.

We also show numerical results for the case when the elements of $\mathbf{W}_\mathrm{a}$ or $\mathbf{W}_\mathrm{b}$ are BPSK-modulated (i.e., 1 becomes -1, and 0 becomes 1), as proposed in [11]. We then denote these matrices as $\mathbf{W}_{\mathrm{a,BPSK}}$ or $\mathbf{W}_{\mathrm{b,BPSK}}$. Note that the BPSK modulation of $\mathbf{W}$ is not related to the modulation of the transmitted symbol s.

Let us assume that, beside $\widehat{\mathbf{h}}_\mathrm{p}$, the receiver knows also $\mathbf{W}$ (i.e., $\mathbf{W}_\mathrm{a}$ or $\mathbf{W}_\mathrm{b}$). Let us also assume that the columns of $\mathbf{W}$ are normalized. Then, the columns of $\mathbf{W}$ can be employed for an optimum combining approach herein denoted 'binary MRC'. Its steps, for independent and identically distributed (i.i.d.) Rayleigh fading, are as follows:

1) Determine the (normalized) column of $\mathbf{W}$ that maximizes symbol-detection SNR, as follows:
$$\mathbf{w}_{\mathrm{MRC,binary}} = arg \max_{\mathbf{w}_i \in \mathbf{W}} |\mathbf{w}_i^{\mathcal{H}} \widehat{\mathbf{h}}_\mathrm{p}|, \tag{21}$$
which requires N inner products.
2) Isolate the 'phase' of $\mathbf{h} \cdot s$ with the inner product
$$\mathbf{w}_{\mathrm{MRC,binary}}^{\mathcal{H}} \mathbf{y}. \tag{22}$$
3) Isolate the 'phase' of $\mathbf{h}$ with the inner product
$$\mathbf{w}_{\mathrm{MRC,binary}}^{\mathcal{H}} \widehat{\mathbf{h}}_\mathrm{p}. \tag{23}$$
4) Estimate symbol s by mapping
$$\widehat{s}_{\mathrm{MRC,binary}} = \frac{1}{\sqrt{E_\mathrm{s}}} \frac{\mathbf{w}_{\mathrm{MRC,binary}}^{\mathcal{H}} \mathbf{y}}{\mathbf{w}_{\mathrm{MRC,binary}}^{\mathcal{H}} \widehat{\mathbf{h}}_\mathrm{p}} \tag{24}$$
into the modulation constellation. Note that, unlike for conventional MRC, binary MRC requires the denominator term $\mathbf{w}_{\mathrm{MRC,binary}}^{\mathcal{H}} \widehat{\mathbf{h}}_\mathrm{p}$ even for PSK-modulated s.

For correlated Rayleigh fading we can write $\mathbf{h} = \mathbf{R}^{1/2} \mathbf{h}_\mathrm{w}$, where $\mathbf{h}_\mathrm{w}$ is an i.i.d., zero-mean, unit-variance, complex-valued Gaussian vector. Then, we employ the channel gain correlation matrix to modify the matrix with the binary MRC combiners as follows

$$\mathbf{W}_{\text{corr. Rayleigh}} = \mathbf{R}^{1/2} \mathbf{W}, \tag{25}$$

based on a previous proposal for MIMO precoding [13].

Similarly, for correlated Rician fading we can transform our binary combiners either using information only about the AS with (25) or by using information about the K, $\mathbf{h}_\mathrm{d}$, and AS with

$$\mathbf{W}_{\text{corr. Rician}} = \mathbf{C}^{1/2} \mathbf{W}. \tag{26}$$

Note that binary MRC requires that the receiver maintains $\mathbf{R}^{1/2}$ or $\mathbf{C}^{1/2}$. On the other hand, the operations required to compute (25) or (26) are very simple for binary $\mathbf{W}$.

IV. Numerical Results

We now describe simulation results for the MRC methods presented above. The simulation settings are as follows: Rayleigh and Rician fading ($K = 7$ dB); BPSK modulation; 300 000 samples of BPSK symbol, channel, and noise; uniform linear array (ULA) receive antenna with $N_\mathrm{R} = 4$ and normalized interelement distance $d_\mathrm{n} = 1$ (i.e., actual distance equal to half of the carrier wavelength); Laplacian PAS with central AOA $\theta_\mathrm{c} = 0$, LOS AOA $\theta_{\mathrm{LOS}} = 0$ (unless specified otherwise)[1], AS $= 2°$ (unless specified otherwise); spatial correlation computed from $d_\mathrm{n} = 1$, $\theta_\mathrm{c} = 0$, and AS as in [15, Eqns. (4.3),(4.4)].

[1]These angles are measured with respect to the line perpendicular on the ULA

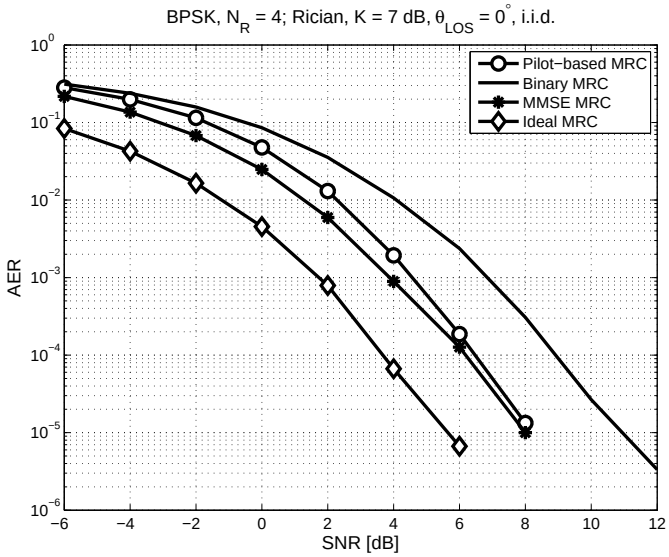

Fig. 1. Simulated MRC AER vs. SNR, for Rician i.i.d. fading with $K = 7$ dB, BPSK, $N_{\mathrm{R}} = 4$, and $\mathbf{W}_{\text{corr. Rician}}$ derived from unmodulated $\mathbf{W}_{\mathrm{b}}$.

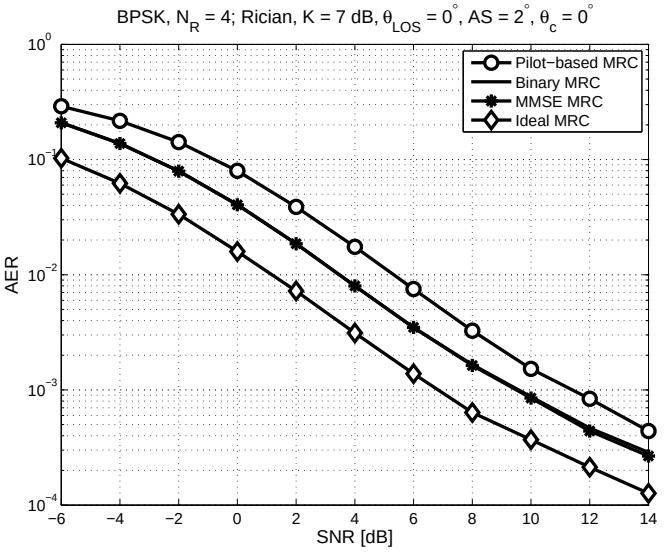

Fig. 2. Simulated MRC AER vs. SNR, for Rician fading with $K = 7$ dB and AS $= 2^{\circ}$, BPSK, $N_{\mathrm{R}} = 4$, and $\mathbf{W}_{\text{corr. Rician}}$ derived from unmodulated $\mathbf{W}_{\mathrm{b}}$.

In most of the figures described below, the horizontal axis represents is the SNR, i.e., E_{s}/N_0, and the vertical axis represents the average symbol error rate (AER) obtained by numerical simulation.

Fig. 1 depicts the i.i.d. Rician fading case whereby binary MRC employs $\mathbf{W}_{\text{corr. Rician}}$ and unmodulated $\mathbf{W}_{\mathrm{b}}$. Note that even simple pilot-based MRC outperforms binary MRC over the entire SNR range. Nevertheless, binary MRC appears to yield the same diversity order as conventional MRC. On the other hand, MMSE MRC substantially outperforms simple pilot-based MRC at low SNR. At high SNR, they yield similar performance, which is expected, because $\mathbf{G}$ from (16) then becomes $\mathbf{I}_{N_{\mathrm{R}}}$, and thus $\mathbf{w}_{\text{MRC,MMSE}} = \mathbf{w}_{\text{MRC,pilot}} = \widehat{\mathbf{h}}_{\mathrm{p}}$.

Fig. 2 depicts the MRC performance for Rician fading with $\theta_{\mathrm{c}} = \theta_{\mathrm{LOS}} = 0$ and AS $= 2^{\circ}$. Such a low AS value yields significant antenna correlation [15, p. 138] [6]. The figure reveals that MMSE-MRC-like performance is achievable with binary MRC. Recall that the latter does not require the inversion of a matrix (which may be inaccurate, at high correlation).

Fig. 3 reveals the effect of BPSK-modulating $\mathbf{W}_{\mathrm{b}}$ on binary MRC performance.[2] Note that such modulation was proposed for binary precoders in [11]. The figure reveals that binary MRC is now outperformed even by simple pilot-based MRC. Therefore, hereafter we employ only unmodulated $\mathbf{W}$.

Results not shown here have revealed that unmodulated $\mathbf{W}_{\mathrm{b}}$ and $\mathbf{W}_{\mathrm{a}}$ yield similar binary-MRC performance when $\theta_{\mathrm{c}} = \theta_{\mathrm{LOS}} = 0$. On the other hand, for $\theta_{\mathrm{c}} \neq \theta_{\mathrm{LOS}}$, Fig. 4 reveals that, at high-SNR, $\mathbf{W}_{\mathrm{a}}$ can significantly outperform $\mathbf{W}_{\mathrm{b}}$. The plot identified by $\mathbf{I}_4$ is explained shortly.

Let us now consider Rician fading with combiner matrix

[2]Note that BPSK-modulated $\mathbf{W}_{\mathrm{a}}$ would yield the same performance because $\mathbf{W}_{\mathrm{a}} = [\mathbf{W}_{\mathrm{b}}, -\mathbf{W}_{\mathrm{b}}]$, and thus its second half reduces to the first half by the absolute-value operation in (21). On the other hand, unmodulated $\mathbf{W}_{\mathrm{a}}$ and $\mathbf{W}_{\mathrm{b}}$ do not yield the same performance, as shown later.

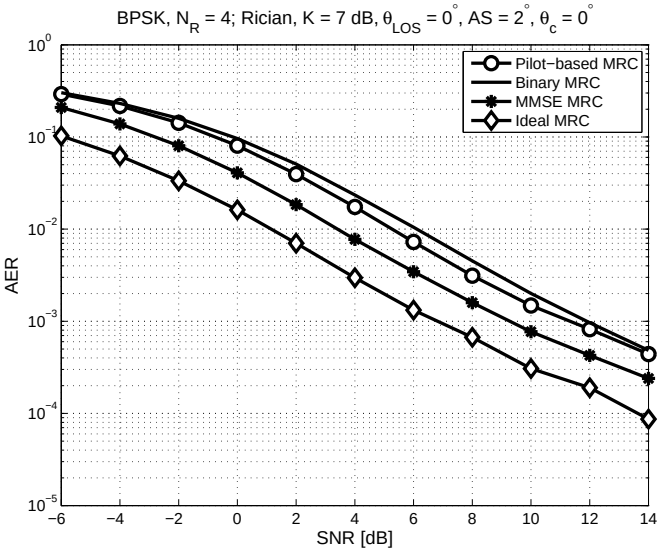

Fig. 3. Simulated MRC AER vs. SNR, for Rician fading with $K = 7$ dB and AS $= 2^{\circ}$, BPSK, $N_{\mathrm{R}} = 4$, and $\mathbf{W}_{\text{corr. Rician}}$ with $\mathbf{W}_{\text{b,BPSK}}$.

$\mathbf{W}_{\text{corr. Rician}}$ computed with (26) from unmodulated $\mathbf{W}$. Then, the column with index i of $\mathbf{W}_{\text{corr. Rician}}$ that is selected by (21) corresponds to the column with index i of the binary $\mathbf{W}$. Fig. 5 shows the histograms of these column indexes, revealing that certain binary combiners from $\mathbf{W}_{\mathrm{b}}$ and $\mathbf{W}_{\mathrm{a}}$ (in fact, the corresponding combiners from $\mathbf{W}_{\text{corr. Rician}}$) are selected more frequently than others. For example, for $\mathbf{W}_{\mathrm{b}}$ from (19), columns $2, 3, 5$ are selected for more than 80% of the channel samples. On the other hand, for $\mathbf{W}_{\mathrm{a}}$ from (19) and (20), columns $2, 3, 5, 9$ are selected for more than 70% of the channel samples. Note that these contain a single 1 entry. Note also that column 5 is selected twice more often for $\mathbf{W}_{\mathrm{b}}$ than for

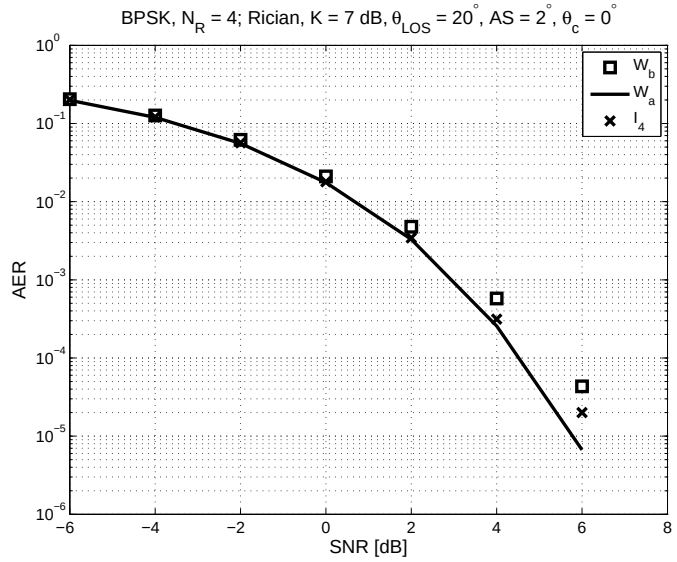

Fig. 4. Simulated binary-MRC AER vs. SNR, for Rician fading with $K = 7$ dB and AS $= 2^\circ$, $\theta_\mathrm{c} = 0$, $\theta_\mathrm{LOS} = 20^\circ$, $N_\mathrm{R} = 4$, and $\mathbf{W}_{\text{corr. Rician}}$ derived from unmodulated $\mathbf{W}_\mathrm{b}$, $\mathbf{W}_\mathrm{a}$, and $\mathbf{I}_4$.

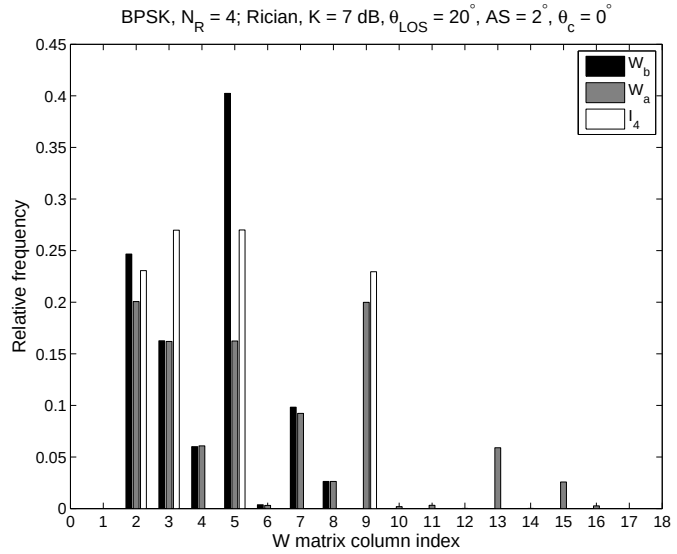

Fig. 5. Histograms of the index of selected $\mathbf{W}_{\text{corr. Rician}}$ (unmodulated $\mathbf{W}$) column, for $E_\mathrm{s}/N_0 = 14$ dB, Rician fading with $K = 7$ dB and AS $= 2^\circ$, $\theta_\mathrm{c} = 0$, $\theta_\mathrm{LOS} = 20^\circ$, $N_\mathrm{R} = 4$.

$\mathbf{W}_\mathrm{a}$. Finally, note that, for $\mathbf{W}_\mathrm{a}$, columns $9 - 16$ are selected for about 30% of the channel samples. Their absence from $\mathbf{W}_\mathrm{b}$ renders the performance with $\mathbf{W}_\mathrm{b}$ worse than with $\mathbf{W}_\mathrm{a}$, as shown in Fig. 4. The absence of column 9 (with a single 1 entry) from $\mathbf{W}_\mathrm{b}$ is particularly significant, as this column is selected with $\mathbf{W}_\mathrm{a}$ for about 20% of the channel samples.

When the binary approach is applied for maximal-ratio transmission (MRT) [10] for correlated Rician fading and limited transmit–receive feedback [13], we can exploit the fact that some of the combiners are selected more frequently

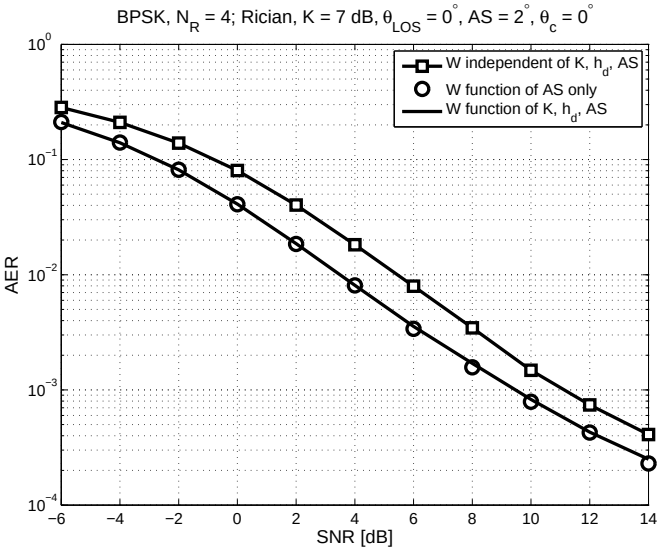

Fig. 6. Simulated binary-MRC AER vs. SNR, for Rician fading with $K = 7$ dB and AS $= 2^\circ$, $N_\mathrm{R} = 4$, and various choices of $\mathbf{W}$ derived from unmodulated $\mathbf{W}_\mathrm{a}$.

than others as follows. Instead of assigning to all codebook beamformers the same number of bits for their codebook indices, we propose to assign shorter codes to the more frequently selected beamformers and longer codes to the less frequently selected beamformers. This approach, inspired by the source coding concept, is currently under study.

Lets us now return to our numerical results for SIMO binary MRC. Fig. 5 also shows the histogram for the combiner matrix $\mathbf{W}$ formed with the 4 columns of $\mathbf{W}_\mathrm{a}$ with a single 1 entry. Since $\mathbf{W}$ is then a permutation of the $\mathbf{I}_4$ identity matrix, the columns of $\mathbf{W}_{\text{corr. Rician}}$ are simply the columns of $\mathbf{C}^{1/2}$. Back in Fig. 4 we show that, at high SNR, the low-dimension and simple combiner matrix $\mathbf{I}_4$ outperforms $\mathbf{W}_\mathrm{b}$ and underperforms $\mathbf{W}_\mathrm{a}$. Hereafter, we show results only for unmodulated $\mathbf{W}_\mathrm{a}$.

Fig. 6 reveals a negligible difference in the performance of binary MRC for $\mathbf{W}$ computed as a function of AS only with (25), or as a function of K, $\mathbf{h}_\mathrm{d}$, and AS with (26). On the other hand, using the untransformed binary $\mathbf{W}$ yields significantly poorer performance. These results would suggest that accounting only for spatial correlation in designing the binary-MRC weight matrix is sufficient. However, other results (not shown here) have revealed that, for $\theta_\mathrm{c} \neq \theta_\mathrm{LOS}$, $\mathbf{W}$ computed with (25) renders binary MRC useless, whereas $\mathbf{W}$ computed with (26) still helps binary MRC achieve nearly the same AER as MMSE MRC, at least for low SNR.

Fig. 7 shows results for Rayleigh fading, $\mathbf{W}_{\text{corr. Rayleigh}}$ derived from unmodulated $\mathbf{W}_\mathrm{a}$ with (25), and otherwise the same settings as for Fig. 2, which depicts Rician fading. Note that binary MRC still performs close to MMSE MRC, but only for low-to-medium SNR.

Fig. 8 shows that binary MRC can extract extra diversity gain induced by specular propagation. Therefore, for SIMO,

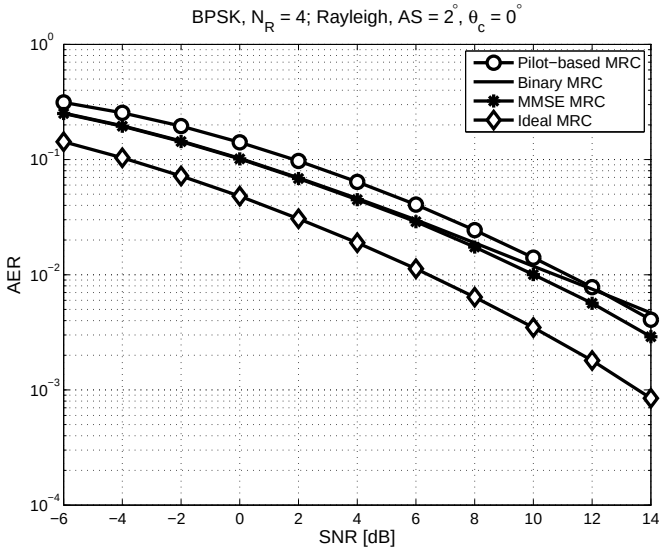

Fig. 7. Simulated MRC AER vs. SNR, for Rayleigh fading with AS $= 2^\circ$, $N_\mathrm{R} = 4$, and $\mathbf{W}_{\text{corr. Rayleigh}}$ derived from (25) with unmodulated $\mathbf{W}_\mathrm{a}$.

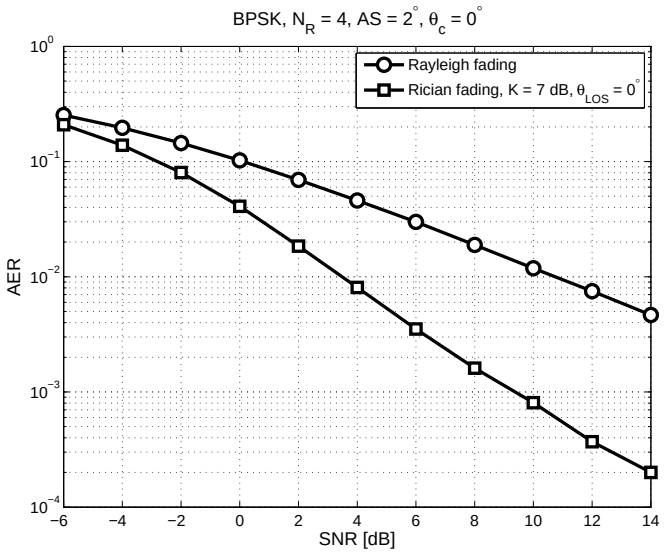

Fig. 8. Simulated binary-MRC AER vs. SNR, for Rician fading with $K = 7$ dB and for Rayleigh fading, both with AS $= 2^\circ$, $N_\mathrm{R} = 4$, $\mathbf{W}_{\text{corr. Rayleigh}}$ derived with (25), $\mathbf{W}_{\text{corr. Rician}}$ derived with (26) from unmodulated $\mathbf{W}_\mathrm{a}$.

Rician fading yields better performance than Rayleigh fading even with binary MRC.

V. Conclusions

We have shown that binary MRC can achieve near-optimum performance for Rician fading, high channel correlation (i.e., low AS), and non-high SNR. We found that BPSK-modulating the binary combiner matrix, as proposed previously, is not effective for SIMO MRC. Instead we have employed a $0/1$-valued binary combiner matrix. We have also found that the combiner matrix with all binary combinations performs best. On the other hand, because of missing a crucial combiner, a previously-proposed combiner matrix is outperformed even by the identity matrix. We are currently attempting to analyze binary MRC mathematically, in order to derive average error probability expressions. Future work will investigate whether binary MRC has lower memory storage and computational requirements than conventional approaches. Then, binary MRC may be suitable in OFDM systems, to simplify combining on the many subcarriers. Future work will also attempt to generalize the binary-transceiver concept to MIMO.

References

[1] A. J. Paulraj, R. U. Nabar, and D. A. Gore, *Introduction to Space-Time Wireless Communications*. Cambridge, UK: Cambridge University Press, 2003.

[2] C. Siriteanu, S. D. Blostein, and J. Millar, "FPGA-based communications receivers for smart antenna array embedded systems," *EURASIP Journal on Embedded Systems. Special Issue on Field-Programmable Gate Arrays in Embedded Systems*, vol. 2006, pp. Article ID 81 309, 13 pages, 2006.

[3] A. Burg, "VLSI circuits for MIMO communication systems," Ph.D. dissertation, Swiss Federal Institute of Tech., 2006.

[4] W. Gabran and B. Daneshrad, "Hardware and physical layer adaptation for a power constrained MIMO OFDM system," in *Proc. IEEE International Conference on Communications, (ICC '11)*, 2011.

[5] D. Love, R. Heath, V. Lau, D. Gesbert, B. Rao, and M. Andrews, "An overview of limited feedback in wireless communication systems," *IEEE Journal on Selected Areas in Communications*, vol. 26, no. 8, pp. 1341 –1365, October 2008.

[6] C. Siriteanu and S. D. Blostein, "Maximal-ratio eigen-combining for smarter antenna arrays," *IEEE Transactions on Wireless Communications*, vol. 6, no. 3, pp. 917 – 925, March 2007.

[7] C. Siriteanu, Y. Miyanaga, and S. D. Blostein, "Evaluation of SIMO eigencombining for estimated and correlated Rician fading," *Journal on Wireless Communications and Networking, submitted*, July 2011.

[8] C. Siriteanu, X. Shi, and Y. Miyanaga, "MIMO zero-forcing detection performance for correlated and estimated Rician fading with lognormal azimuth spread and K-factor," in *IEEE Int. Conf. on Communications, (ICC'11), Kyoto, Japan*, June 2011.

[9] ——, "Analysis and simulation of MIMO zero-forcing detection performance for correlated and estimated Rician fading," *IEEE Transactions on Vehicular Technology, submitted*, July 2011.

[10] T. Lo, "Maximum ratio transmission," *IEEE Transactions on Communications*, vol. 47, no. 10, pp. 1458 –1461, October 1999.

[11] Y. G. Kim and N. Beaulieu, "Binary Grassmannian weightbooks for MIMO beamforming systems," *IEEE Transactions on Communications*, vol. 59, no. 2, pp. 388–394, February 2011.

[12] P. Kyosti, J. Meinila, L. Hentila, and *et al.*, "WINNER II Channel Models." CEC, Tech. Rep. IST-4-027756, 2008.

[13] D. Love and J. Heath, R.W., "Limited feedback diversity techniques for correlated channels," *IEEE Transactions on Vehicular Technology*, vol. 55, no. 2, pp. 718 – 722, March 2006.

[14] M. K. Simon and M.-S. Alouini, *Digital Communication Over Fading Channels. A Unified Approach to Performance Analysis*. Baltimore, Maryland: John Wiley and Sons, 2000.

[15] C. Siriteanu, "Maximal-ratio eigen-combining for smarter antenna array wireless communication receivers," Ph.D. dissertation, Queen's University, Kingston, Canada, 2006.

[16] V. Erceg, P. Soma, D. S. Baum, and S. Catreux, "Multiple-input multiple-output fixed wireless radio channel measurements and modeling using dual-polarized antennas at 2.5 GHz," *IEEE Transactions on Wireless Communications*, vol. 3, no. 6, pp. 2288 – 2298, November 2004.

[17] C. Siriteanu, G. Xin, and S. D. Blostein, "Performance and complexity comparison of MRC and PASTd-based statistical beamforming and eigencombining," in *14th Asia–Pacific Conf. on Communications (APCC'08), Tokyo, Japan*, 2008.

[18] J. G. Proakis, *Digital Communications*, 4th ed. New York, NY: McGraw-Hill, Inc., 2001.